ORGANOMETALLICS

Article

Cite This: *Organometallics* 2019, 38, 1286–1291

pubs.acs.org/Organometallics

pH-Dependent Reactivity of a Water-Soluble Nickel Complex: Hydrogen Evolution vs Selective Electrochemical Hydride Generation

Charlene Tsay, Bianca M. Ceballos, and Jenny Y. Yang*

Department of Chemistry, University of California, Irvine, California 92697, United States

Supporting Information

ABSTRACT: Mechanistic details for the aqueous hydrogen evolution reaction (HER) electrocatalyst $[Ni(DHMPE)_2]^{2+}$ (DHMPE = 2-bis(bis(hydroxymethyl)phosphino)ethane) are reported. The proposed $2e^-$ reduced catalytic intermediate $[Ni(DHMPE)_2]$ was added to solutions between pH 1 and 5. The two sequential protonation events leading to H_2 evolution were monitored by $^{31}P\{^1H\}$ NMR spectroscopy. The initial protonation event to generate the metal hydride $[HNi(DHMPE)_2]^+$ proceeds to completion within 1.5 min. In contrast, significant variation in the pH-dependent rate and reaction progress of the second protonation event to form the H−H bond is observed. The differences are discussed in the context of the free energy of each protonation event, which also defines the pH conditions under which H_2 evolution is exergonic. The analysis provides useful information on the functional pH range of HER electrocatalysts that proceed through metal hydride intermediates. Reductive electrolysis of $[Ni(DHMPE)_2]^{2+}$ under conditions in which H_2 evolution is endergonic (pH 7) leads to selective generation of the corresponding metal hydride $[HNi(DHMPE)_2]^+$. The electrolytic generation of a kinetically competent reducing metal hydride intermediate with minimal H_2 evolution illustrates a route for accessing selective reduction of non-proton substrates.

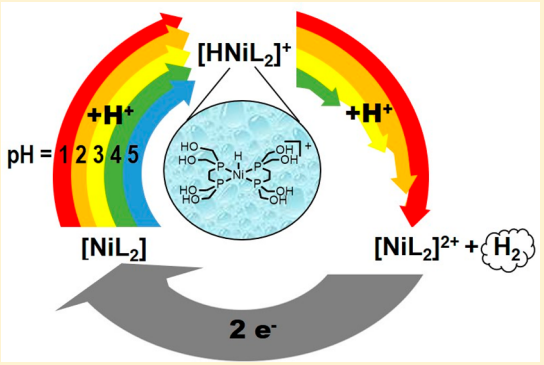

INTRODUCTION

The electrocatalytic reduction of feedstock chemicals to fuels is an important step toward converting renewable electricity into a medium more suitable for energy storage and transportation applications.[1] Proton reduction from water is a focal point for electrocatalytic fuel generation because hydrogen can be used directly as a fuel or as a chemical reductant.[2] As a result, there has been robust interest in developing and understanding aqueous electrocatalysts for the hydrogen evolution reaction (HER).[3]

We recently reported the complex $[Ni(DHMPE)_2]^{2+}$ (DHMPE = 2-bis(bis(hydroxymethyl)phosphino)ethane) (**1**) (Chart 1). $[Ni(DHMPE)_2]^{2+}$ (**1**) is a robust and active electrocatalyst for proton reduction at pH 1, a common operating condition in commercial electrolyzers.[3k] Our proposed mechanism is shown in Chart 1. In water, dimethyl sulfoxide (DMSO), and acetonitrile, $[Ni(DHMPE)_2]^{2+}$ (**1**) exhibits a $2e^-$ irreversible reduction to $[Ni(DHMPE)_2]$ (**2**). In our prior study, various acid sources were utilized in DMSO to demonstrate stepwise generation of the metal hydride $[HNi(DHMPE)_2]^+$ (**3**) followed by protonation to evolve H_2.[3k]

In this study, we investigated the pH-dependent mechanism of aqueous hydrogen evolution. The rate and degree of completion for each protonation step are discussed in the context of its thermodynamic free energy. The results illustrate how hydricity,[4] or the heterolytic cleavage energy of the metal hydride (**3**), determines the functional range for favorable H_2 evolution.

The assessment of conditions under which H_2 evolution is exergonic also implicitly defines conditions under which it is suppressed. Electrolytic generation of reducing metal hydride intermediates provides a route for the selective reduction of

Chart 1. Proposed Electrocatalytic Cycle for $[Ni(DHMPE)_2]^{2+}$ (Left) and Thermochemical Properties for the Intermediate Hydride $[HNi(DHMPE)_2]^+$ (Right)

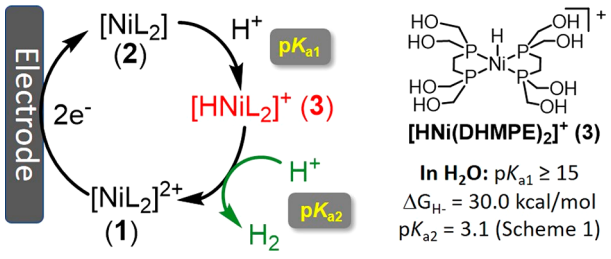

Special Issue: Organometallic Electrochemistry: Redox Catalysis Going the Smart Way

Received: August 2, 2018
Published: October 8, 2018

DOI: 10.1021/acs.organomet.8b00558
Organometallics 2019, 38, 1286–1291

nonprotic substrates. To this end, we demonstrate the selective electrolytic generation of the metal hydride intermediate ($[HNi(DHMPE)_2]^+$ (**3**) in Chart 1) from $[Ni(DHMPE)_2]^{2+}$ (**1**) at pH 7 with little or no H_2 evolution under both aqueous conditions and DMSO.

RESULTS AND DISCUSSION

Metal Hydride Formation and pH-Dependent Hydrogen Evolution. Each nickel species in the proposed catalytic cycle shown in Chart 1 has been independently synthesized and characterized.[5] **1**−**3** are all diamagnetic with diagnostic ^{31}P NMR signatures in acetonitrile and DMSO. **1**−**3** are all soluble in water, but **2** has never been observed, as it rapidly protonates to generate **3** (vide infra). However, **2** can be synthesized in tetrahydrofuran or CH_3CN and isolated as a solid. $^{31}P\{^1H\}$ NMR spectroscopy was used to directly monitor the two sequential protonation reactions upon dissolution of **2** in water to first generate the metal hydride (**3**) and then evolve H_2 to regenerate the resting state catalyst (**1**).

The reduced complex $[Ni(DHMPE)_2]$ (**2**) was added to aqueous buffered solutions between pH 1 and 5. The solutions consist of a 10-fold excess of buffer so that proton activity does not change significantly over the course of the experiment.

The first $^{31}P\{^1H\}$ NMR spectrum was taken at 1.5 min and every 2.5 min thereafter for 75 min. The first protonation to generate $[HNi(DHMPE)_2]^+$ (**3**) (singlet at 54 ppm) is rapid at all pH values and the initial Ni(0) species (**2**) is never observed under these conditions. The spectra over 75 min at pH 2.5 are shown in Figure 1; compiled spectra for all other pH values are shown in Figures S1−S8.

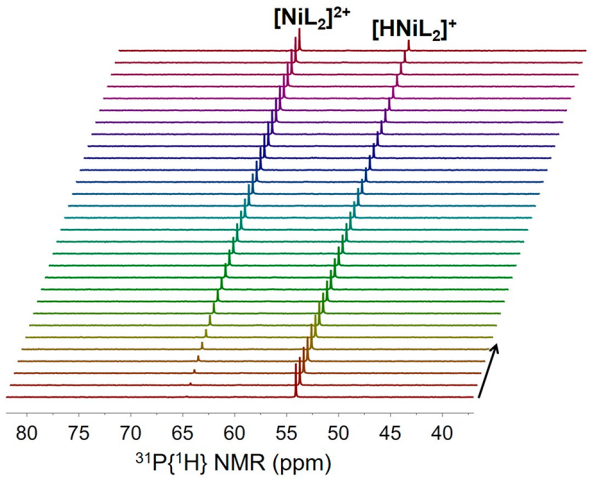

Figure 1. $^{31}P\{^1H\}$ NMR spectra displaying protonation of $[HNi(DHMPE)_2]^+$ (**3**) (singlet at 54 ppm) to release H_2 and generate $[Ni(DHMPE)_2]^{2+}$ (**1**) (singlet at 65 ppm) at pH 2.5 over time (spectra were recorded every 2.5 min for 75 min, from bottom to top). Time-resolved spectra between pH 1 and 5 are shown in Figures S1−S8.

The second protonation event with the metal hydride (**3**) results in H−H bond formation and generation of the four-coordinate Ni(II) species $[Ni(DHMPE)_2]^{2+}$ (**1**) (singlet at 65 ppm). The $^{31}P\{^1H\}$ NMR spectra contained an internal standard to confirm the total amount of nickel hydride complex (**3**) and Ni(II) complex (**1**) is conserved (there are no decomposition or off-cycle reaction pathways).

Figure 2 shows the concentrations of **3** (dashed) and **1** (solid) over 75 min, color coded by pH. At pH 1, both protonation events occur within 4 min. Between pH 1.5 and 5, protonation occurs more slowly before the concentrations of **3** and **1** approach stable values. The reaction progress (K) is described by the relative concentrations of the resting state (**1**) after H_2 evolution and the nickel hydride (**3**) (or [**1**]/[**3**]). After 75 min, the reaction progress (K) for protonation of the metal hydride (**3**) to evolve H_2 ranges from ∼27 to 10^{-2} for this reaction from pH 1.5 through 4.5 (see Table 1). K declines with increasing pH values. Above pH 3 the reaction proceeds to less than 50% completion after 75 min. At pH 5 no protonation is observed after 75 min—only the metal hydride (**3**) is found in solution.

Kinetics of Protonation. The first protonation step to generate nickel hydride (**3**) is rapid and is never observed between pH 1 and 5. We were unable to discern quantitative rates for the formation of **3** using electrochemical techniques because of the nonideal irreversible $2e^-$ reduction of **1** in the cyclic voltammogram. However, we note that rates of protonation to generate cobalt and nickel hydride complexes have been reported using systems that were more ideally suited for kinetic studies.[6]

In contrast to the first protonation event, the second protonation event is observed at all pH values, indicating that the latter is slower. In aqueous solutions, electrochemical reduction of **1** is under diffusion control, indicating that electron transfer is rapid.[3k] Thus, protonation of the metal hydride to form the H−H bond is likely the rate-determining step during catalysis.

Analysis of the initial rate between pH 1.5 and 4.5 indicates a first-order reaction with respect to proton concentration (see Figure S9). An initial rate constant (k_{obs}) was determined at each pH, and the values are given in Table S1. Protonation occurs very rapidly at the low pH values, limiting the data available for kinetic analysis. At pH 1, only one spectrum is obtained before the reaction is complete; therefore, the calculated observed rate represents a lower bound. No protonation of the metal hydride (**3**) is observed at pH 5 after 75 min. The relationship between log k_{obs} for H_2 evolution and pH is shown in Figure 3.

Thermodynamic Considerations of Metal Hydride Formation and Hydrogen Evolution. The pH-dependent reaction progress given in Table 1 and kinetic relationships (Figure 3) can be contextualized with regard to the free energy of the protonation reactions. The free energies of the first and second protonation steps are dependent on the pK_a and hydricity, respectively, of the metal hydride. The pK_a value of $[HNi(DHMPE)_2]^+$ is ≥15 in water.[5] The first protonation step in Chart 1 is exergonic under all of the conditions we examined (pH 1−5).

The free energy of the second protonation to evolve hydrogen (eq 4 in Scheme 1) is dictated by the hydricity of the metal hydride (eq 1), the proton activity (or pH) of the reaction conditions (eq 2), and the solvent-dependent heterolytic bond cleavage energy of H_2 (eq 3). This relationship is depicted at the bottom of Scheme 1. The hydricity of $[HNi(DHMPE)_2]^+$ was measured to be 30.0 kcal/mol in water[5] and is represented by the dashed red line in Scheme 1. The calculated ΔG values for H_2 evolution under the standard state conditions of 1 atm of H_2 for each pH condition of our study are shown in Table 1. From this analysis, we see that protonation to evolve H_2 is thermoneutral

DOI: 10.1021/acs.organomet.8b00558
Organometallics 2019, 38, 1286−1291

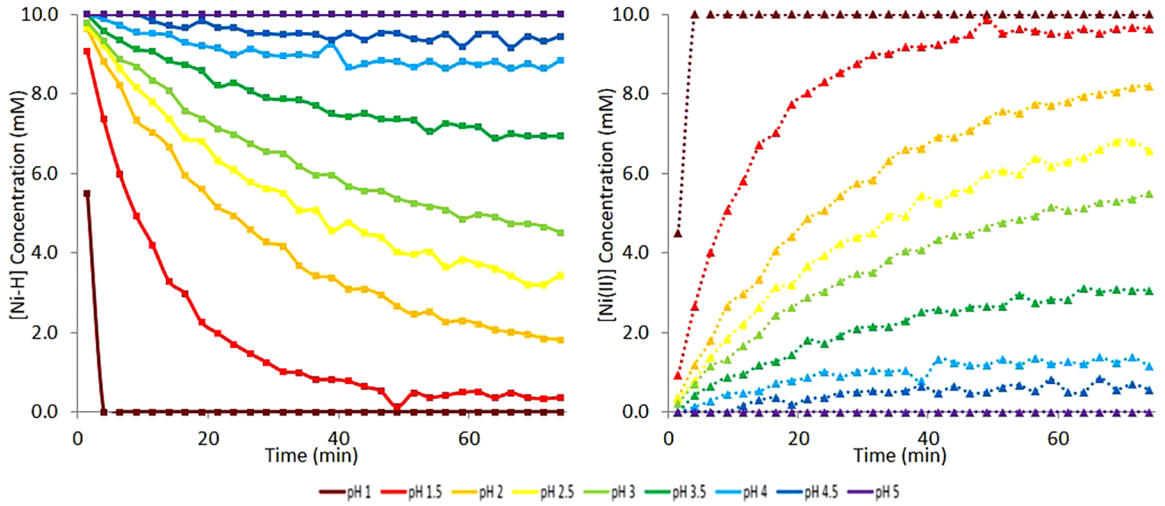

Figure 2. Concentration of $[HNi(DHMPE)_2]^+$ (**3**) (left, solid lines with squares) and $[Ni(DHMPE)_2]^{2+}$ (**1**) (right, dashed lines with triangles) after dissolution of $Ni(DHMPE)_2$ (**2**) in aqueous solutions between pH 1 and 5, recorded every 2.5 min over 75 min. Concentrations were measured by normalizing the integrated $^{31}P\{^1H\}$ NMR peaks of each species; comparison to a capillary integration standard confirms quantitative conversion from **3** to **1**.

Table 1. Free Energy of Protonation of $[HNi(DHMPE)_2]^+$ (3) To Release H_2 and Generate $[Ni(DHMPE)_2]^{2+}$ (1) from pH 1 through 5 (from Eq 4 in Scheme 1 under 1 atm of H_2) and Measured *K* after 75 min under 1 atm of N_2 Using $^{31}P\{^1H\}$ NMR Spectroscopy

pH	*K* ([**1**]/[**3**]) (under 1 atm N_2)	calcd ΔG (kcal/mol, under 1 atm H_2)
1	no **3** obsd	−2.83
1.5	26.7	−2.15
2	4.53	−1.46
2.5	1.92	−0.78
3	1.22	−0.09
3.5	0.44	0.60
4	0.13	1.28
4.5	0.06	1.97
5	0.00	2.65

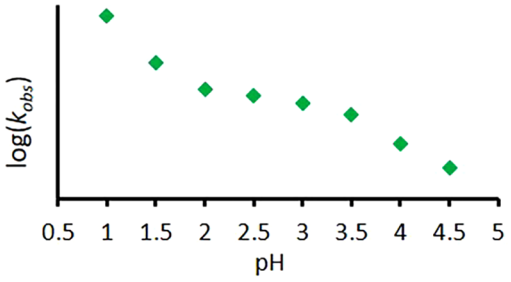

Figure 3. log k_{obs} vs pH for H_2 formation at pH 1−5 on the basis of ^{31}P NMR spectroscopic data. The k_{obs} value at pH 1 represents a lower bound (see main text).

Scheme 1. (Top) Thermodynamic Cycle Describing H_2 Formation by Heterocoupling (or Protonation) of a Metal Hydride Intermediate and (Bottom) Thermochemistry of Metal Hydride Protonation (Eq 4) by Hydricity and pH Used to Determine pK_{a2}[a]

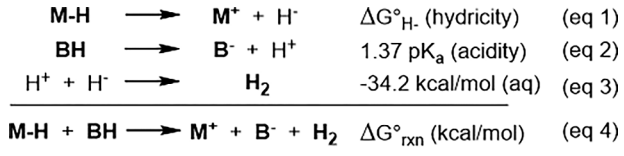

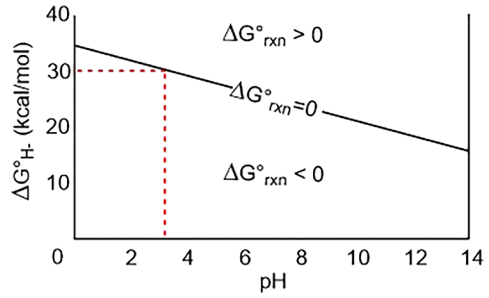

[a]The dashed red line is drawn for the hydricity of $[HNi(DHMPE)_2]^+$ in H_2O (ΔG_{H^-} = 30 kcal/mol).

at pH 3.1 (i.e., pK_{a2} = 3.1). H_2 evolution is exergonic at lower pH values and endergonic above it.

The standard state for eq 4 (Scheme 1) is 1 atm of H_2. Our NMR experiments were carried out under 1 atm of N_2 instead of 1 atm of H_2 to replicate conditions used in catalytic hydrogen production. Despite the change in atmosphere, we find reaction progress after 75 min, at which point the concentration of **3** and **1** is only minimally changing, is consistent with the free energy calculated for the reaction. When the free energy of protonation becomes positive, the ratio [**1**]/[**3**] falls below 1 as expected. Additionally, the extent to which the reaction proceeds decreases about 1 order of magnitude per increase in pH unit, which is consistent with the change in free energy.

The pH-dependent free energy of protonation to deliver H_2 also provides insight into the observed rate. The plot of log k_{obs} vs pH illustrates a decline in rate that correlates with the free energy of the reaction. A linear free energy relationship with proton activity has previously been observed with nickel and cobalt hydrides under conditions in which H_2 evolution is exergonic.[7] The log k_{obs} value shows a dependence on pH that decreases as the reaction approaches thermoneutral conditions. At higher pH values, log k_{obs} slows in a linear fashion until pH 5, when no appreciable protonation is observed. Thus, the rate

DOI: 10.1021/acs.organomet.8b00558
Organometallics 2019, 38, 1286−1291

decreases as the thermodynamic driving force for H_2 formation decreases, with an apparent inflection around where protonation is thermoneutral ($\Delta G = 0$).

We attempted to measure rates of electrocatalytic H_2 evolution at higher pH values. However, lower proton activities requires high scan rates to achieve pure kinetic conditions, at which point we observe diffusion-controlled processes from $[Ni(DHMPE)_2]^{2+}$ reduction due to slowing catalytic rates. Nevertheless, our kinetic data for the rate-determining step indicate that the rate of H_2 evolution decreases with increasing pH.

Selective Electrolytic Generation of Metal Hydride. *Under Aqueous Conditions.* Transition-metal hydrides are also important intermediates in a broad range of reduction reactions.[4,8] Metal hydride intermediates for reduction chemistry are most commonly accessed using hydrogen and a base or a hydride donor. Performing these reductions through electrolysis would minimize the use of sacrificial reductants by generating metal hydride using electrons from an electrode and protons from solution. However, parasitic H_2 evolution in solutions that contain protons can undermine Faradaic efficiency or product yield in comparison to total current passed and presents a major challenge in reductive electrolysis.[9]

The thermodynamic analysis described above also provides valuable information on how to suppress H_2 evolution while maintaining sufficient proton activity to generate a metal hydride. This information provides an entry point to achieving selective reduction of non-proton substrates, an approach that has been successful for both heterogeneous[10] and homogeneous catalysts.[11]

Controlled-potential electrolysis of $[Ni(DHMPE)_2]^{2+}$ was performed under various conditions to demonstrate isolation of the corresponding hydride after aqueous electrolysis (electrolysis cell is shown in Figure S10). In all of the controlled-potential electrolysis experiments (under H_2 or N_2), the products were quantified against an internal standard by $^{31}P\{^1H$ NMR$\}$ to ensure that the total amount of nickel complex was conserved (no degradation was observed in the postelectrolysis solutions). We demonstrated in our prior study that no changes in electrolytic behavior occur upon addition of elemental mercury, and no residual compound was observed after rinsing the electrode.[3k] Both experiments indicate that these nickel complexes are not prone to decomposition or; at absorption onto the electrode. We also previously determined that the nickel hydride (**2**) is stable with respect to homolytic H_2 evolution.[3k]

An electrolysis of **1** was performed under 1 atm H_2 in a pH 7 buffered (glycinamide) solution of $[Ni(DHMPE)_2]^{2+}$ (Figure S11; at this pH, ΔG value of H_2 evolution is 5.3 kcal/mol according to eq 4 in Scheme 1). Upon electrolysis at −0.8 V vs SHE (about 270 mV beyond the two-electron reduction potential of $[Ni(DHMPE)_2]^{2+}$) and passing of a little more than 2 equiv of charge, $[HNi(DHMPE)_2]^+$ (**3**) is the *only* species observed in solution (Figure 4, middle). We note that this electrolysis was performed under 1 atm of H_2 to be consistent with the thermodynamics of protonation described in eq 4. While performing electrolysis under 1 atm of H_2 may be practical for achieving selective reduction for products that remain in solution, it is less desirable for reactions that produce gaseous products.

Therefore, we repeated the electrolysis of **1** under the same conditions (pH 7) except under 1 atm of N_2 (Figure S12).

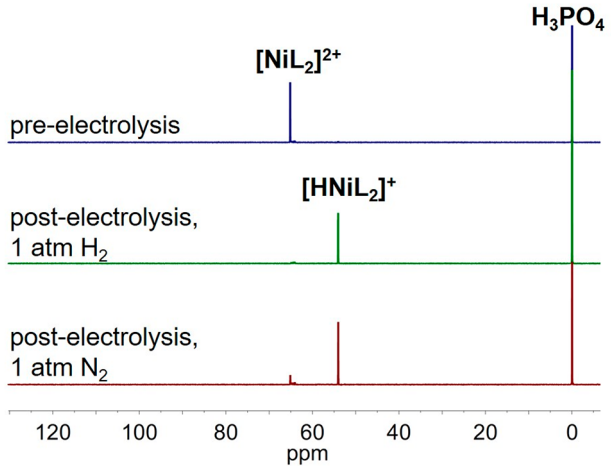

Figure 4. $^{31}P\{^1H\}$ NMR spectra of $[Ni(DHMPE)_2]^{2+}$ (**1**) before (blue, top) and after electrolysis at −0.8 V vs SHE at pH 7 for 7 h under 1 atm of H_2 (green, middle) and 1 atm of N_2 (red, bottom).

After a similar amount of charge was passed, $[HNi(DHMPE)_2]^+$ and $[Ni(DHMPE)_2]^{2+}$ were both present in the postelectrolysis solution in a nearly 7/1 ratio (Figure 4, bottom). Additionally, when the sealed headspace of the electrolysis was analyzed, only ∼0.6 equiv of hydrogen (with respect to nickel) was detected. Although operation under a non-H_2 atmosphere leads to some protonation of the hydride to form H_2, a high concentration of $[HNi(DHMPE)_2]^+$ was still isolable after electrolysis. This result demonstrates that $[HNi(DHMPE)_2]^+$ can be generated as a kinetically competent intermediate under electrolytic conditions.

In Dimethyl Sulfoxide (DMSO). Although all of the conditions described thus far have focused on aqueous catalysis, the thermodynamic cycle in Scheme 1 is also applicable to other solvent systems, provided the appropriate hydricity (eq 1), pK_a scale (eq 2), and heterolytic bond cleavage energy of H_2 (eq 3) for that solvent is used. Since the thermochemical properties of $[HNi(DHMPE)_2]^+$ (**3**) in DMSO have been measured, we utilized the data to determine conditions for selective electrochemical generation.

In DMSO the hydricity of **3** is 55.5 kcal/mol[5] and the pK_a is 9.26.[5] Using the heterolytic bond cleavage energy of H_2 (60.7 kcal/mol in DMSO),[12] the pK_{a2} value where hydrogen evolution is thermoneutral (from Scheme 1) is calculated to be 3.8. Therefore, tri-*n*-butylammonium ($[HNBu_3]^+$, pK_a = 8.4 in DMSO)[13] is sufficiently acidic to generate **3** from the reduced complex **2** without resulting in significant protonation of **3** to form H_2. After a solution of $[Ni(DHMPE)_2]^{2+}$ underwent controlled-potential electrolysis at (−2.0 V vs $Fe(C_5H_5)_2^{+/0}$, Figure S13) in the presence of 10 equiv of $[HNBu_3]^+$ under an N_2 atmosphere, only $[HNi(DHMPE)_2]^+$ was observed in the postelectrolysis $^{31}P\{^1H\}$ NMR spectrum (Figure S14).

CONCLUSION

The hydrogen evolution activity of electrocatalyst $[Ni(DHMPE)_2]^{2+}$ (**1**) was previously described at pH 1. This study investigated the pH-dependent reactivity of the $2e^-$ reduced proposed intermediate $[Ni(DHMPE)_2]$ (**2**) using $^{31}P\{^1H\}$ NMR spectroscopy. Dissolution of **2** in aqueous solutions between pH 1 and 5 permits investigation into both protonation reactions prior to H_2 evolution. The first

DOI: 10.1021/acs.organomet.8b00558
Organometallics 2019, 38, 1286−1291

protonation to generate the metal hydride $[HNi(DHMPE)_2]^+$ (**3**) rapidly proceeds to completion in this pH range, and **2** is never observed. The rate and extent of protonation of the metal hydride to evolve H_2 at each pH was correlated to the free energy of that reaction, which can be calculated using the hydricity of **3**.

Conversely, the hydricity can also be utilized to determine conditions under which the metal hydride $[HNi(DHMPE)_2]^+$ is stable to protonation and thus can be electrochemically generated and isolated. We demonstrate the electrolytic generation of kinetically competent $[HNi(DHMPE)_2]^+$ (**3**) in water and DMSO. We believe this type of analysis provides a possible route to accessing metal hydride intermediates for selective electrochemical reduction of non-proton substrates.

Our analysis supports the importance of quantifying hydricity to rationalize reactivity and as a consideration in catalyst design. While most hydricity values were initially measured in organic solvents, particularly acetonitrile,[4,14] more recent work has focused on aqueous values[15] or solvent dependence.[5,16] We believe these quantitative studies are valuable to advancing our understanding of metal hydride reactivity and reductive catalysis.

■ ASSOCIATED CONTENT

Supporting Information

The Supporting Information is available free of charge on the ACS Publications website at DOI: 10.1021/acs.organomet.8b00558.

Experimental details, NMR data, controlled-potential electrolyses, and pre- and post-electrolysis analyses (PDF)

■ AUTHOR INFORMATION

Corresponding Author

*E-mail for J.Y.Y.: j.yang@uci.edu.

ORCID

Jenny Y. Yang: 0000-0002-9680-8260

Notes

The authors declare no competing financial interest.

■ ACKNOWLEDGMENTS

This material is based on work supported by the U.S. Department of Energy, Office of Science, Office of Basic Energy Sciences under Award Number DE-SC0012150. B.M.C. was also supported by a National Science Foundation Graduate Research Fellowship under Grant No. DGE# 1321846. JYY is also grateful for support as a Sloan Foundation Fellow and a CIFAR Azrieli Global Scholar.

■ REFERENCES

(1) (a) Lewis, N. S.; Nocera, D. G. Powering the planet: Chemical challenges in solar energy utilization. *Proc. Natl. Acad. Sci. U. S. A.* **2006**, *103* (43), 15729−15735. (b) Song, W.; Chen, Z.; Brennaman, M. K.; Concepcion, J. J.; Patrocinio, A. O. T.; Iha, N. Y. M.; Meyer, T. J. Making solar fuels by artificial photosynthesis. *Pure Appl. Chem.* **2011**, *83* (4), 749−768. (c) Gust, D.; Moore, T. A.; Moore, A. L. Solar Fuels via Artificial Photosynthesis. *Acc. Chem. Res.* **2009**, *42* (12), 1890−1898.

(2) (a) Turner, J. A. Sustainable Hydrogen Production. *Science* **2004**, *305* (5686), 972−974. (b) Bard, A. J.; Fox, M. A. Artificial Photosynthesis: Solar Splitting of Water to Hydrogen and Oxygen. *Acc. Chem. Res.* **1995**, *28* (3), 141−145. (c) Pagliaro, M.; Konstandopoulos, A. G.; Ciriminna, R.; Palmisano, G. Solar hydrogen: fuel of the near future. *Energy Environ. Sci.* **2010**, *3* (3), 279−287. (d) Graetzel, M. Artificial photosynthesis: water cleavage into hydrogen and oxygen by visible light. *Acc. Chem. Res.* **1981**, *14* (12), 376−384. (e) Crabtree, G. W.; Dresselhaus, M. S. The Hydrogen Fuel Alternative. *MRS Bull.* **2008**, *33* (4), 421−428.

(3) (a) Thoi, V. S.; Sun, Y.; Long, J. R.; Chang, C. J. Complexes of earth-abundant metals for catalytic electrochemical hydrogen generation under aqueous conditions. *Chem. Soc. Rev.* **2013**, *42* (6), 2388−2400 and references therein . (b) Kandemir, B.; Kubie, L.; Guo, Y.; Sheldon, B.; Bren, K. L. Hydrogen Evolution from Water under Aerobic Conditions Catalyzed by a Cobalt ATCUN Metallopeptide. *Inorg. Chem.* **2016**, *55* (4), 1355−1357. (c) Kleingardner, J. G.; Kandemir, B.; Bren, K. L. Hydrogen Evolution from Neutral Water under Aerobic Conditions Catalyzed by Cobalt Microperoxidase-11. *J. Am. Chem. Soc.* **2014**, *136* (1), 4−7. (d) Zee, D. Z.; Chantarojsiri, T.; Long, J. R.; Chang, C. J. Metal−Polypyridyl Catalysts for Electro- and Photochemical Reduction of Water to Hydrogen. *Acc. Chem. Res.* **2015**, *48* (7), 2027−2036. (e) Nguyen, A. D.; Rail, M. D.; Shanmugam, M.; Fettinger, J. C.; Berben, L. A. Electrocatalytic Hydrogen Evolution from Water by a Series of Iron Carbonyl Clusters. *Inorg. Chem.* **2013**, *52* (21), 12847−12854. (f) Wang, Z.-Q.; Tang, L.-Z.; Zhang, Y.-X.; Zhan, S.-Z.; Ye, J.-S. Electrochemical-driven water splitting catalyzed by a water-soluble cobalt(II) complex supported by N,N′-bis(2′-pyridinecarboxamide)-1,2-benzene with high turnover frequency. *J. Power Sources* **2015**, *287*, 50−57. (g) Eckenhoff, W. T.; Brennessel, W. W.; Eisenberg, R. Light-Driven Hydrogen Production from Aqueous Protons using Molybdenum Catalysts. *Inorg. Chem.* **2014**, *53* (18), 9860−9869. (h) Halter, D. P.; Heinemann, F. W.; Bachmann, J.; Meyer, K. Uranium-mediated electrocatalytic dihydrogen production from water. *Nature* **2016**, *530* (7590), 317−321. (i) Halter, D. P.; Palumbo, C. T.; Ziller, J. W.; Gembicky, M.; Rheingold, A. L.; Evans, W. J.; Meyer, K. Electrocatalytic H2O Reduction with f-Elements: Mechanistic Insight and Overpotential Tuning in a Series of Lanthanide Complexes. *J. Am. Chem. Soc.* **2018**, *140* (7), 2587−2594. (j) Koshiba, K.; Yamauchi, K.; Sakai, K. A Nickel Dithiolate Water Reduction Catalyst Providing Ligand-Based Proton-Coupled Electron-Transfer Pathways. *Angew. Chem.* **2017**, *129* (15), 4311−4315. (k) Tsay, C.; Yang, J. Y. Electrocatalytic Hydrogen Evolution under Acidic Aqueous Conditions and Mechanistic Studies of a Highly Stable Molecular Catalyst. *J. Am. Chem. Soc.* **2016**, *138* (43), 14174−14177. (l) Xue, D.; Peng, Q.-X.; Zhan, S.-Z. Synthesis and electrochemical properties of a water soluble nickel(II) complex supported by N-phenylpyridin-2-ylmethanimine ligand. *Inorg. Chem. Commun.* **2017**, *82*, 11−15.

(4) Wiedner, E. S.; Chambers, M. B.; Pitman, C. L.; Bullock, R. M.; Miller, A. J. M.; Appel, A. M. Thermodynamic Hydricity of Transition Metal Hydrides. *Chem. Rev.* **2016**, *116* (15), 8655−8692.

(5) Tsay, C.; Livesay, B. N.; Ruelas, S.; Yang, J. Y. Solvation Effects on Transition Metal Hydricity. *J. Am. Chem. Soc.* **2015**, *137* (44), 14114−14121.

(6) (a) Elgrishi, N.; Kurtz, D. A.; Dempsey, J. L. Reaction Parameters Influencing Cobalt Hydride Formation Kinetics: Implications for Benchmarking H2-Evolution Catalysts. *J. Am. Chem. Soc.* **2017**, *139* (1), 239−244. (b) Wiedner, E. S.; Brown, H. J. S.; Helm, M. L. Kinetic Analysis of Competitive Electrocatalytic Pathways: New Insights into Hydrogen Production with Nickel Electrocatalysts. *J. Am. Chem. Soc.* **2016**, *138* (2), 604−616. (c) Rountree, E. S.; Dempsey, J. L. Potential-Dependent Electrocatalytic Pathways: Controlling Reactivity with pKa for Mechanistic Investigation of a Nickel-Based Hydrogen Evolution Catalyst. *J. Am. Chem. Soc.* **2015**, *137* (41), 13371−13380.

(7) (a) Rountree, E. S.; Dempsey, J. L. Reactivity of Proton Sources with a Nickel Hydride Complex in Acetonitrile: Implications for the Study of Fuel-Forming Catalysts. *Inorg. Chem.* **2016**, *55* (10), 5079−5087. (b) Rountree, E. S.; Martin, D. J.; McCarthy, B. D.; Dempsey, J. L. Linear Free Energy Relationships in the Hydrogen Evolution Reaction: Kinetic Analysis of a Cobaloxime Catalyst. *ACS Catal.* **2016**, *6* (5), 3326−3335.

DOI: 10.1021/acs.organomet.8b00558
Organometallics 2019, 38, 1286−1291

(8) Eberhardt, N. A.; Guan, H. Nickel Hydride Complexes. *Chem. Rev.* **2016**, *116* (15), 8373−8426.
(9) (a) Inglis, J. L.; MacLean, B. J.; Pryce, M. T.; Vos, J. G. Electrocatalytic pathways towards sustainable fuel production from water and CO2. *Coord. Chem. Rev.* **2012**, *256* (21−22), 2571−2600. (b) Seh, Z. W.; Kibsgaard, J.; Dickens, C. F.; Chorkendorff, I.; Nørskov, J. K.; Jaramillo, T. F. Combining theory and experiment in electrocatalysis: Insights into materials design. *Science* **2017**, *355* (6321), eaad4998.
(10) Li, C. W.; Ciston, J.; Kanan, M. W. Electroreduction of carbon monoxide to liquid fuel on oxide-derived nanocrystalline copper. *Nature* **2014**, *508*, 504−507.
(11) (a) Elgrishi, N.; Chambers, M. B.; Fontecave, M. Turning it off! Disfavouring hydrogen evolution to enhance selectivity for CO production during homogeneous CO2 reduction by cobalt-terpyridine complexes. *Chemical Science* **2015**, *6* (4), 2522−2531. (b) Fogeron, T.; Todorova, T. K.; Porcher, j. p.; Gomez-Mingot, M.; Chamoreau, L.-M.; Mellot-Draznieks, C.; Li, Y.; Fontecave, M. A Bioinspired Nickel(bis-dithiolene) Complex as a Homogeneous Catalyst for Carbon Dioxide Electroreduction. *ACS Catal.* **2018**, *8* (3), 2030−2038.
(12) Wayner, D. D. M.; Parker, V. D. Bond energies in solution from electrode potentials and thermochemical cycles. A simplified and general approach. *Acc. Chem. Res.* **1993**, *26* (5), 287−294.
(13) Kolthoff, I. M.; Chantooni, M. K.; Bhowmik, S. Dissociation constants of uncharged and monovalent cation acids in dimethyl sulfoxide. *J. Am. Chem. Soc.* **1968**, *90* (1), 23−28.
(14) (a) Berning, D. E.; Noll, B. C.; DuBois, D. L. Relative Hydride, Proton, and Hydrogen Atom Transfer Abilities of [HM-(diphosphine)2]PF6 Complexes (M = Pt, Ni). *J. Am. Chem. Soc.* **1999**, *121* (49), 11432−11447. (b) Rakowski Dubois, M.; Dubois, D. L. Development of Molecular Electrocatalysts for CO2 Reduction and H2 Production/Oxidation. *Acc. Chem. Res.* **2009**, *42* (12), 1974−1982. (c) Yang, J. Y.; Bullock, R. M.; DuBois, M. R.; DuBois, D. L. Fast and efficient molecular electrocatalysts for H2 production: Using hydrogenase enzymes as guides. *MRS Bull.* **2011**, *36* (1), 39−47. (d) Lilio, A. M.; Reineke, M. H.; Moore, C. E.; Rheingold, A. L.; Takase, M. K.; Kubiak, C. P. Incorporation of Pendant Bases into Rh(diphosphine)2 Complexes: Synthesis, Thermodynamic Studies, And Catalytic CO2 Hydrogenation Activity of [Rh(P2N2)2]+ Complexes. *J. Am. Chem. Soc.* **2015**, *137* (25), 8251−8260.
(15) (a) Brereton, K. R.; Bellows, S. M.; Fallah, H.; Lopez, A. A.; Adams, R. M.; Miller, A. J. M.; Jones, W. D.; Cundari, T. R. Aqueous Hydricity from Calculations of Reduction Potential and Acidity in Water. *J. Phys. Chem. B* **2016**, *120* (50), 12911−12919. (b) Pitman, C. L.; Brereton, K. R.; Miller, A. J. M. Aqueous Hydricity of Late Metal Catalysts as a Continuum Tuned by Ligands and the Medium. *J. Am. Chem. Soc.* **2016**, *138* (7), 2252−2260. (c) Burgess, S. A.; Kendall, A. J.; Tyler, D. R.; Linehan, J. C.; Appel, A. M. Hydrogenation of CO2 in Water Using a Bis(diphosphine) Ni−H Complex. *ACS Catal.* **2017**, *7* (4), 3089−3096.
(16) (a) Brereton, K. R.; Pitman, C. L.; Cundari, T. R.; Miller, A. J. M. Solvent-Dependent Thermochemistry of an Iridium/Ruthenium H2 Evolution Catalyst. *Inorg. Chem.* **2016**, *55* (22), 12042−12051. (b) Loewen, N. D.; Neelakantan, T. V.; Berben, L. A. Renewable Formate from C−H Bond Formation with CO2: Using Iron Carbonyl Clusters as Electrocatalysts. *Acc. Chem. Res.* **2017**, *50* (9), 2362−2370. (c) Taheri, A.; Thompson, E. J.; Fettinger, J. C.; Berben, L. A. An Iron Electrocatalyst for Selective Reduction of CO2 to Formate in Water: Including Thermochemical Insights. *ACS Catal.* **2015**, *5* (12), 7140−7151. (d) Ceballos, B. M.; Tsay, C.; Yang, J. Y. CO2 reduction or HCO2- oxidation? Solvent-dependent thermochemistry of a nickel hydride complex. *Chem. Commun.* **2017**, *53* (53), 7405−7408. (e) Burgess, S. A.; Appel, A. M.; Linehan, J. C.; Wiedner, E. S. Changing the Mechanism for CO2 Hydrogenation Using Solvent-Dependent Thermodynamics. *Angew. Chem., Int. Ed.* **2017**, *56* (47), 15002−15005.

DOI: 10.1021/acs.organomet.8b00558
Organometallics 2019, 38, 1286−1291